Polymorphism of a New Bis(ethylenedithio)tetrathiafulvalene (BEDT-TTF) Based Molecular Conductor; Novel Transformations in Metallic BEDT-TTF Layers

ARTICLE *in* CHEMISTRY OF MATERIALS · JUNE 2004

Impact Factor: 8.35 · DOI: 10.1021/cm034866q

Polymorphism of a New Bis(ethylenedithio)tetrathiafulvalene (BEDT-TTF) Based Molecular Conductor; Novel Transformations in Metallic BEDT-TTF Layers

Elena Laukhina,*[,†,‡] Vladeslava Tkacheva,[‡] Aleksandr Chekhlov,[‡] Eduard Yagubskii,[‡] Roman Wojciechowski,[§] Jacek Ulanski,[§] Jose Vidal-Gancedo,[†] Jaume Veciana,[†] Vladimir Laukhin,[†,||] and Concepció Rovira*[,†]

Institut de Ciència de Materials de Barcelona CSIC, Campus UAB, E-08193 Bellaterra, Spain, Institute of Problems of Chemical Physics, RAS, MD, 142432, Chernogolovka, Russia, Department of Molecular Physics, Faculty of Chemistry, Technical University of Lódz, ul. Zeromskiego 116, 90-924 Lódz, Poland, and Institució Catalana de Recerca i Estudis Avançats (ICREA)

Received September 16, 2003. Revised Manuscript Received March 19, 2004

The synthesis, structure, anion composition, and physical properties of a new organic conductor (BEDT-TTF)$_2$[(IBr$_2$)$_{0.2}$(BrICl)$_{0.1}$(ICl$_2$)$_{0.7}$], where BEDT-TTF = bis(ethylenedithio)-tetrathiafulvalene, are described in detail. This molecular conductor exists as two polymorphs displaying semiconducting (β'-phase) and metallic (β''-phase) transport properties. Complete β'' to β and partial β'' to β' transformation have been discovered for the first time in conducting BEDT-TTF-based salts and studied by using ESR spectroscopy. Both transformations are irreversible, the $\beta'' \rightarrow \beta$ one resulting from high-temperature solid-state reactions. The β''- and β-phases are variable in composition.

Introduction

Synthetic metals based on trihalide salts of bis-(ethylenedithio)tetrathiafulvalene (BEDT-TTF)[1−4] are of great interest due to their unique physical properties and their high sensitivity to chemical modifications. These features make them very attractive as model molecular conductors of reduced dimensionality.[5−10] It should be stressed that BEDT-TTF trihalide salts can be successfully generated as a continuous well-oriented nanocrystalline layer at the surface of a polymeric film that allows one to combine the transport and magnetic properties of molecular conductors with the advantageous properties of commercial polymers.[11,12]

Recently we reported some new and important examples of BEDT-TTF-based organic conductors that can contain different sets of various trihalide anions.[4,9,12,13] Among them there is the unique molecular conductor (BEDT-TTF)$_2$Br$_{1.3}$I$_{1.1}$Cl$_{0.6}$ that switches between a metallic state, which is stable at low and high temperatures, and a semiconductor state, which is stable at intermediate temperatures.[9,13] This phenomenon was a new finding in molecular organic crystals and might be used in a number of applications.

In general, the transport properties of BEDT-TTF salts depend on the structure of the BEDT-TTF radical-

* To whom correspondence should be addressed. E-mail: laukhina@icmab.es (E.L.) and cun@icmab.es (C.R.).
† Institut de Ciència de Materials de Barcelona CSIC.
‡ Institute of Problems of Chemical Physics, RAS.
§ Technical University of Lódz.
|| ICREA.

(1) Shibaeva, R. P.; Kaminskii, V. F.; Yagubskii, E. B. *Mol. Cryst. Liq. Cryst.* **1985**, *119*, 361.
(2) Shibaeva, R. P.; Yagubskii, E. B.; Laukhina, E. E.; Laukhin, V. N. In *The Physics and Chemistry of Organic Superconductors*; Saito, G., Kagishima, S., Eds.; Springer-Verlag: Heidelberg, FRG, 1990; p 342.
(3) Williams, J. M.; Ferraro, J. R.; Thorn, R. J.; Carlson, K. D.; Geiser, U.; Wang, H. H.; Kini, A. M.; Whangbo, M.-H. *Organic Superconductors (Including Fullerenes): Synthesis, Structure, Properties, and Theory*; Prentice Hall: Englewood Cliffs, NJ, 1992.
(4) Laukhina, E. E.; Narymbetov, B. Zh.; Zorina, L. V.; Khasanov, S. S.; Rozenberg, L. P.; Shibaeva, R. P.; Buravov, L. I.; Yagubskii, E. B.; Avramenko, N. V.; Van, K. *Synth. Met.* **1997**, *90*, 101.
(5) Saito, G. In *Organic Molecular Solids*; Jones, W., Ed.; CRC Press: Boca Raton, FL, 1997; Chapter 10.
(6) Laukhin, V. N.; Kostyjuchenko, E. E.; Sushko, Yu. V.; Shchegolev, I. F.; Yagubskii, E. B. *JETP Lett.* **1985**, *41*, 68.
(7) Baran, G. O.; Buravov, L. I.; Degtyarev L. S.; Kozlov, M. E.; Laukhin, V. N.; Laukhina, E. E.; Onishchenko, V. G.; Pokhodnya, K. I.; Sheinkman, M. K.; Shibaeva, R. P.; Yagubskii, E. B. *Pis'ma Zh. Eksp. Teor. Fiz. (USSR)* **1986**, *44*, 293; *JETP Lett. (USA)* **1986**, *44*, 376 (English translation).
(8) Avramenko, N. V.; Zvarykina, A. V.; Laukhin, V. N.; Laukhina, E. E.; Lubovskii, R. B.; Shibaeva, R. P. *JETP Lett. (USA)* **1988**, *48*, 472 (English translation).
(9) Laukhina, E.; Vidal-Gancedo, J.; Khasanov, S.; Tkacheva, V.; Zorina, L.; Shibaeva, R.; Singleton, J.; Wojciechowski, R.; Ulanski, J.; Laukhin, V.; Veciana, J.; Rovira, C. *Adv. Mater.* **2000**, *12*, 1205.
(10) Bender, K.; Dietz, K.; Endres, H.; Helberg, H. W.; Henning, I.; Keller, H. J.; Schafer, H. W.; Scheitzer, D. *Mol. Cryst. Liq. Cryst.* **1984**, *107*, 45.
(11) Laukhina, E. E.; Ulanski, J.; Khomenko, A. G.; Pesotskii, S. I.; Tkachev, V.; Atovmyan, L.; Yagubskii, E. B.; Rovira, C.; Veciana, J.; Vidal-Gancedo J.; Laukhin, V. *J. Phys. I Fr.* **1997**, *7*, 1665.
(12) Laukhina, E.; Tkacheva, V.; Chuev, I.; Yagubskii, E.; Vidal-Gancedo, J.; Mas-Torrent, M.; Rovira, C.; Veciana, J.; Khasanov, S.; Wojciechowski, R.; Ulanski, J. *J. Phys. Chem. B* **2001**, *105*, 11089.
(13) Laukhina, E.; Vidal-Gancedo, J.; Laukhin, V.; Veciana, J.; Chuev, I.; Tkacheva, V.; Wurst, K.; Rovira, C. *J. Am. Chem. Soc.* **2003**, *125*, 3948.

10.1021/cm034866q CCC: $27.50
Published on Web 05/11/2004

Table 1. Experimental Data on the Synthesis of the New $(BEDT\text{-}TTF)_2[(IBr_2)_{0.2}(BrICl)_{0.1}(ICl_2)_{0.7}]$ Salt

method	reagents, mmol: BEDT-TTF	reagents, mmol: salt **1**	NB, mL	aspect	crystal type	phase
A	0.26	1.25	40	needles	2	β'
				plates	3	β''
B	0.05	0.1	20	plates	4	β''

cation layers that alternate with layers of anions.[3,5,14,15] In the presence of very weak contact interactions between BEDT-TTF molecules such as S···S and C−H···C, the C−H···Y−I−Y$^-$ (Y = Br, Cl) interactions are crucial in determining the packing of the BEDT-TTF radical-cations and hence govern the conducting properties of the BEDT-TTF trihalide salts.[3,16] Therefore, the in-depth study of BEDT-TTF based salts, which contain various sets of different trihalide anions, can shed light on the relationship between a fine adjustment of the structure of the BEDT-TTF layer by the C−H···Y−I−Y$^-$ (Y = I, Br, Cl) interactions and macroscopic properties of BEDT-TTF trihalide salts.

Here we present a systematic study of the polymorphism of the new $(BEDT\text{-}TTF)_2[(IBr_2)_{0.2}(BrICl)_{0.1}(ICl_2)_{0.7}]$ molecular conductor. This BEDT-TTF-based salt was prepared in order to study two problems: (i) to know which kind of BEDT-TTF trihalides can be formed from solutions containing different sets of trihalide anions and (ii) to study how macroscopic properties of BEDT-TTF trihalides might depend on a collection of the C−H···Y−I−Y$^-$ (Y = Br, Cl) interactions.

Experimental Section

Synthesis of the $Me_4N[(IBr_2)_{0.2\pm\delta}(BrICl)_{0.1\pm\delta}(ICl_2)_{0.7\pm\delta}]$ Salt. The salt was synthesized using Me_4NBr and ICl as initial reagents. At 50 °C, 1.55 g (10 mmol) of Me_4NBr was dissolved in 30 mL of acetone. Then, under stirring, 3.3 g (20 mmol) of ICl was added to the acetone solution and the reagent mixture was cooled to room temperature. As a result, small yellow crystals of the $Me_4NBr_{0.5\pm0.1}I_{1.0\pm0.1}Cl_{1.5\pm0.1}$ salt (**1**) were formed. The crystals were filtered off and recrystallized from acetone yielding 2.36 g (80%), T_M = 209 °C.

Preparation of β'- and β''-$(BEDT\text{-}TTF)_2[(IBr_2)_{0.2\pm\delta}(BrICl)_{0.1\pm\delta}(ICl_2)_{0.7\pm\delta}]$ Single Crystals. A. Under argon, salt **1** (470 mg) was added to a solution of BEDT-TTF (100 mg) in nitrobenzene (NB, 40 mL) at 120 °C (see Table 1). The mixture was cooled to 25 °C with a cooling rate of 1 °C/h. As a result, two kinds of black, shining crystals, needles (**2**) and plates (**3**) (β'- and β''-phase, respectively), were obtained. The crystals were filtered off and traces of the solvent were removed under vacuum. The total yield of the crystals was 70% (92 mg).

B. Crystals (**4**) were grown at 25 °C in nitrobenzene by the standard electrochemical method using **1** as the electrolyte in a conventional H-shaped cell with Pt electrodes. After 1 week, at a constant current of 0.9 μA, a small quantity of black, platelike crystals were obtained and characterized as the β''-phase (Table 1). Notice that at lower values of currents crystals were grown very slowly and after 3−4 weeks they were still too small to be well characterized.

Characterization of Crystals. Energy dispersion X-ray spectroscopy (EDX) analysis was performed with a scanning electron microscope (SEM) HITACHI S-3000N with an EDX-NORAN instrument. The EDX data are summarized in Table 2.

Table 2. Anion Composition of Crystals 1, 2, 3, and 4 as Determined by EDX Method

$[cation]^+[Br_xI_yCl_z]^-$: crystal type	$[cation]^+$	element composition of the $Br_xI_yCl_z^-$ anion, were $x+y+z=3$: x, $\Delta x = 0.1$	y, $\Delta y = 0.1$	z, $\Delta z = 0.1$
1	$(CH_3)_4N^+$	0.5	1.0	1.5
2	$BEDT\text{-}TTF^{+\bullet}$	0.4	1.0	1.6
3	$BEDT\text{-}TTF^{+\bullet}$	0.5	0.9	1.6
4	$BEDT\text{-}TTF^{+\bullet}$	0.5	1.0	1.5

Table 3. Vibration Frequencies of Low-Frequency Raman Bands in Trihalide Salt

$[cation]^+[Br_xI_yCl_z]^-$: crystal type	$[cation]^+$	vibration mode, cm^{-1} [a]: IBr_2^-	$BrICl^-$	ICl_2^-
1	$(CH_3)_4N^+$	160−173 (m) doublet	232 (w)	261 (s)
2	$BEDT\text{-}TTF^{+\bullet}$	164−173 (m) doublet	234 (w)	260 (s)
3	$BEDT\text{-}TTF^{+\bullet}$	172 (m)	239 (w)	264 (s)
4	$BEDT\text{-}TTF^{+\bullet}$	172 (m)	239 (w)	264 (s)

[a] Relative intensities: s = strong, m = medium, w = weak.

The Raman spectra (see Table 3) of the tetramethylammonium salt as well as of single crystals of **2**, **3**, and **4** were performed at 293 K at ambient pressure using a Jobin-Yvon T64000 Raman microscope spectrometer working in back-scattering mode. The measurements were performed with 632 nm laser lines with 1 cm^{-1} resolution. The Raman spectra of **2**, **3**, and **4** were taken at the (*001*) crystallographic plane, and the incident electric field was polarized approximately along the long axis of the trihalide anions.

X-ray crystal data were collected and analyzed for both crystal types: needles (**2**) and plates (**3**). The results obtained showed that the single crystals of **2** and **3** are isostructural to β'- and β''-$(BEDT\text{-}TTF)_2ICl_2$ phases, respectively.[17] The X-ray crystal data collection was performed at room temperature using an Enraf-Nonius CAD-4 diffractometer with graphite-monochromatized Mo Kα radiation (λ = 0.710 69 Å). The main crystal data for needlelike crystal **2** are as follows: a = 6.634(1) Å, b = 9.783(3) Å, c = 12.926(3) Å, α = 87.20(2)°, β = 79.00(2)°, γ = 81.55(2)°, V = 814.4(3) Å^3, space group $P1$, Z = 2, M = 490.21, $d_{calc.}$ = 1.999 g/cm^3. The main crystal data for platelike crystal **3** are as follows: a = 5.757(1) Å, b = 9.029(2) Å, c = 16.290(3) Å, α = 82.80(2)°, β = 96.78(2)°, γ = 103.77(2)°, V = 814.1(3) Å^3, space group $P1$, Z = 2, M = 494.66, $d_{calc.}$ = 2.018 g/cm^3. The intensities of 3911 (for **2**) and 3913 (for **3**) reflections were collected by the $\omega/2\theta$ scan method up to θ_{max} = 28°. The structures were solved by direct methods applying the package SHELXS-97.[18] Both structures were refined by least-squares method in an anisotropic (isotropic for H atoms) approximation using the SHELXL-97 program.[18] A mixed occupation of $(Br_{1-x}Cl_x)$ with identification of the x-parameter was introduced into terminal positions of the BrICl anions. Final agreement factors are R = 0.025 and R = 0.020 for **2** and **3** crystals, respectively. For **2**, the Cl and Br atom occupations were found to be 0.850(2) and 0.150(2) and those for **3** were corresponding to 0.750(2) and 0.250(2), respectively. X-ray study gave the $Br_{0.3}ICl_{1.7}$ anion composition for the β'-crystal and $Br_{0.5}ICl_{1.5}$ for the β''-crystal.

The temperature dependence of resistance of both crystal modifications was measured using the standard four-probe dc-method. Four annealed platinum wires (20 μm in diameter) were attached to a crystal surface by a graphite paste.

(14) Akutsu, H.; Akutsu-Sato, A.; Turner, S. S.; Le Pevelen, D.; Day, P.; Laukhin, V.; Klehe, A.-K.; Singleton, J.; Tocher, D. A.; Probert, M. R.; Howard. J. A. K. *J. Am. Chem. Soc.* **2002**, *124*, 12430.

(15) Deluzet, A.; Rousseau, R.; Guilbaud, Ch.; Granger, I.; Boubekeur, K.; Batail, P.; Canadell, E.; Auban-Senzier, P.; Jerom, D. *Chem. Eur. J.* **2002**, *8*, 3884.

(16) Novoa, J. J.; Mota, F.; Whangbo, M.-H.; Williams, J. M. *Inorg. Chem.* **1991**, *30*, 54.

(17) Buravov, L. I.; Zvarykina, A. V.; Ignat'ev, A. A.; Kotov, A. I.; Laukhin, V. N.; Makova, M. K.; Merzhanov, V. A.; Rozenberg, L. P.; Shibaeva R. P.; Yagubskii, E. B. *Bull. Acad. Sci. USSR (Engl.)* **1988**, 1825.

(18) Sheldrick, G. M. *SHELXL-93, Program for the Refinement of Crystal Structure;* Göttingen University, Germany, 1993.

ESR spectra were recorded using a Bruker ESP-300E spectrometer operating in the X-band (9 GHz) with a rectangular TE_{102} cavity and equipped with a field-frequency (F/F) lock accessory and a built-in Bruker NMR gaussmeter ER 035M. Heating was done at a rate of 1 K/min using a Bruker ER 4121 HT nitrogen cryostat (100−500 K). Rotations were performed by means of a Bruker programmable goniometer ER 218 PGl. Precautions to avoid undesirable spectral line broadening such as that arising from microwave power saturation and magnetic field over-modulation were taken.

The morphology of the conducting surface of the crystals was investigated using a scanning electron microscope (SEM) operating at 20 kV.

Results and Discussion

Synthetic Aspects of the Preparation of the New BEDT-TTF Trihalide Salt. Tetraalkylammonium salts with various inorganic anions are generally used as suppliers of counterions in the preparation of BEDT-TTF salts.[3,5] Moreover, there are syntheses in which tetraalkylammonium salts were successfully used as sources of species that might oxidize BEDT-TTF molecules.[13,19] Therefore, to study the crystallization of BEDT-TTF-based salts from a solution containing IBr_2^-, $BrICl^-$, and ICl_2^- anions, we decided to use a tetraalkylammonium salt possessing a set of these anions. We have suggested the formation of such salts via the $R_4NBr + n$ICl reaction, and indeed, our studies revealed that at $n = 2$, crystals of a new tetraalkylammonium salt (**1**) are formed with a good yield. The composition of **1**, determined by the EDX method (see Table 2), corresponds to $Me_4NBr_{0.5\pm0.1}I_{1.0\pm0.1}Cl_{1.5\pm0.1}$. To clarify the contribution of different trihalide anions, we measured the low-frequency Raman spectrum of **1** (Table 3). The spectrum shows three bands, which correspond to the in-phase stretch vibrations of the IBr_2^-,[20−22] $BrICl^-$,[9,22] and ICl_2^- [21,22] anions, respectively. The band due to the ICl_2^- species is the strongest, in agreement with the halogens' contribution revealed by EDX (see Table 2). Therefore, our study shows that reaction between Br^- and ICl might generate three types of trihalide anions: IBr_2^-, $BrICl^-$, and ICl_2^-.

Taking into account both Raman and EDX data, it is possible to estimate the proportion of trihalide anions. This contribution might vary from $[(IBr_2)_{0.1}(BrICl)_{0.3}(ICl_2)_{0.6}]^-$ to $[(IBr_2)_{0.2}(BrICl)_{0.1}(ICl_2)_{0.7}]^-$. Keeping in mind the intensities of the Raman bands corresponding to IBr_2^- and $BrICl^-$ trihalide anions, the second one is the most credible. In this case, we may ascribe to salt **1** the formula $Me_4N[(IBr_2)_{0.2\pm\delta}(BrICl)_{0.1\pm\delta}(ICl_2)_{0.7\pm\delta}]$, where $\delta < 0.1$. Therefore, for the purposes described in the Introduction, we applied **1** as a source of the mixture of trihalide anions: IBr_2^- (≈20%), $BrICl^-$ (≈10%), and ICl_2^- (≈70%).

Reaction conditions for the chemical oxidation of BEDT-TTF (method A) were similar to those used in the preparation of high-quality crystals of the organic superconductor β-(BEDT-TTF)$_2$IBr$_2$.[19] This method, involving the use of a tetraalkylammonium trihalide in a large excess (Table 1), is based on oxidation of BEDT-TTF by species, such as I_2, IBr, and ICl, which are generated in small amounts in solutions of tetraalkylammonium salts with Y−I−Y$^-$ (Y = I, Br, Cl) anions:

$$RN_4I_3 \rightleftarrows I_2 + I^- + R_4N^+$$

$$RN_4IBr_2 \rightleftarrows IBr + Br^- + R_4N^+$$

$$RN_4ICl_2 \rightleftarrows ICl + Cl^- + R_4N^+$$

With this method, we should take into account not only the formation of monohalide anions (Br^-, Cl^-) but also the generation of new trihalide anions (I_3^-, I_2Br^-, I_2Cl^-) due to the reactions of BEDT-TTF with IY (Y = Br, Cl):[12,23]

$$8\text{BEDT-TTF} + 6\text{IBr} \rightleftarrows [8(\text{BEDT-TTF})]^{+4} + I_3^- + 3IBr_2^-$$

$$8\text{BEDT-TTF} + 6\text{IBr} \rightleftarrows [8(\text{BEDT-TTF})]^{+4} + 2I_2Br^- + 2IBr_2^-$$

$$8\text{BEDT-TTF} + 6\text{ICl} \rightleftarrows [8(\text{BEDT-TTF})]^{+4} + I_3^- + 3ICl_2^-$$

$$8\text{BEDT-TTF} + 6\text{ICl} \rightleftarrows [8(\text{BEDT-TTF})]^{+4} + 2I_2Cl^- + 2ICl_2^-$$

By applying method A we obtained needlelike (**2**) and platelike (**3**) crystals. On the basis of the EDX data, **2** and **3** were found to be (BEDT-TTF)$_2$Br$_{0.4}$I$_{1.0}$Cl$_{1.6}$ and (BEDT-TTF)$_2$Br$_{0.5}$I$_{0.9}$Cl$_{1.6}$, respectively. Since the experimental error in the estimation of the $Br_xI_yCl_z^-$ stoichiometry by the EDX method is ±0.1, we assumed that **2** and **3** are the same BEDT-TTF trihalide salt, the anion composition of which is very close to that of **1**.

By electrocrystallization (method B) using **1** as electrolyte (Table 1) the platelike single crystals of salt **4** were grown. To avoid the chemical reactions described above, we used amounts of **1** smaller than that applied for the chemical oxidation by a factor of 2.5 as well as a much more dilute solution of BEDT-TTF (Table 1).

We reproduced both types of crystallization more than once and tested several crystals from these syntheses. In accordance with the EDX, X-ray, Raman, and ESR data, **4** is identical to **3** (see Experimental Section).

Composition and Structure of BEDT-TTF Trihalides. Below we will analyze Raman spectral data to answer the question of which trihalide anions play a principal role in a formation of the new BEDT-TTF trihalide salt. Figure 1 shows the Raman spectrum of the tetramethylammonium trihalide and the Raman spectra of both types of BEDT-TTF trihalide crystals formed. Because the spectra of **2** and **3** are virtually identical to that of **1**, one may conclude that anion layers of **2** and **3** contain almost the same set of anions as **1**. Therefore, the anion composition of the new BEDT-TTF-based salt can be represented by the following formula $[(IBr_2)_{0.2\pm\delta}(BrICl)_{0.1\pm\delta}(ICl_2)_{0.7\pm\delta}]^-$ ($\delta < 0.1$). This formula gives us an average stoichiometry of $Br_{0.5}I_{1.0}Cl_{1.5}$ for the anion. This result is in excellent agreement with the EDX data, which indicate for the anion composition of

(19) Laukhina, E. E.; Laukhin, V. N.; Khomenko A. G.; Yagubskii, E. B. *Synth. Met.* **1989**, *32*, 88.
(20) Sugai S.; Saito, G. *Solid State Commun.* **1986**, *58*, 759.
(21) Wojciechowski, R.; Ulanski, J.; Lefrant, S.; Faulques, E.; Laukhina, E.; Tkacheva, V. *Synth. Met.* **2000**, *109*, 305.
(22) Wojciekhovski, R.; Ulanski, J.; Lefrant, S.; Faulques, E.; Laukhina, E.; Tkacheva, V. *J. Chem. Phys.* **2000**, *112*, 7634.
(23) Chuev, I. Private communication.

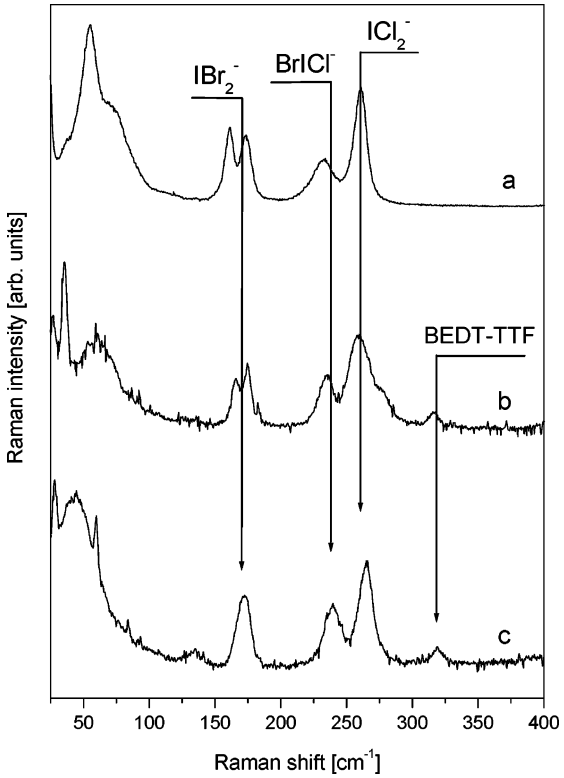

Figure 1. Room-temperature Raman spectra of (a) **1**, (b) **2**, and (c) **3**.

1−**3** a very similar contribution of halides (Table 2). The above formula shows that C−H···Y−I−Y⁻(Y = Br,Cl) interactions from trihalide anions to the CH_2CH_2 groups of BEDT-TTF, which govern the structure of the conducting layer[3,16] of **2** or **3**, consist of (i) C−H···Br−I−Br⁻ interactions formed by [Br−I−Br]⁻ (≈20%) or [Br−I−Cl]⁻ (≈5%) and (ii) C−H···Cl−I−Cl⁻ interactions generated by [Cl−I−Cl]⁻ (≈70%) or [Br−I−Cl]⁻ (≈5%). Therefore, the contribution of the C−H···Br−I−Br⁻ and C−H···Cl−I−Cl⁻ interactions approximates to 25% and 75%, respectively.

It is important to mention that there is a small shift of all considered bands in the spectrum of **2** toward lower frequencies when compared with those of **3** (Figure 1 and Table 3). This effect can be explained by the longer bond lengths in the trihalide anions due to different structural arrangements of **2** and **3**; in that case, **2** and **3** should be two polymorphs of the new BEDT-TTF trihalide salt. X-ray and ESR studies of both types of crystals (needles and plates) fully justify this suggestion (see below). With these results, one may conclude that the above collection of trihalide anions, which is introduced in a large excess in nitrobenzene, is of crucial importance in a formation of crystals **2** or **3**. This is not always the case. For example, the use of the $Bu_4NBr_{0.6}I_{1.4}Cl$ salt generates crystals of BEDT-TTF-based organic conductor with another contribution of halides: $(BEDT\text{-}TTF)_2Br_{1.3}I_{1.1}Cl_{0.6}$.[9]

Below we will focus on X-ray crystal data. Because of geometrical and symmetrical requirements, the relative contribution of the three trihalide species cannot be derived on the basis of the structural data obtained. As noted above, the structure was refined with varying occupancy factors for the terminal Br and Cl atoms. It gave very close composition of anion for **2** and **3** (see Experimental Section) that is in agreement with the contribution of halogens found from the EDX studies (Table 2) within the experimental error of the $Br_xI_yCl_z^-$ stoichiometry determination by both EDX and X-ray methods.

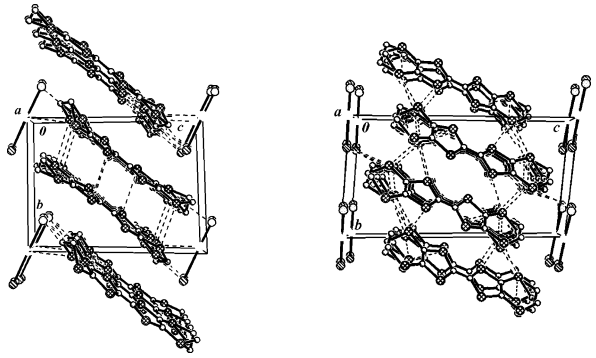

Figure 2. Crystal structure of the $(BEDT\text{-}TTF)_2[(IBr_2)_{0.2}(BrICl)_{0.1}(ICl_2)_{0.7}]$ salt projected along the *a*-axis: (left) *β′*-phase and (right) *β″*-phase

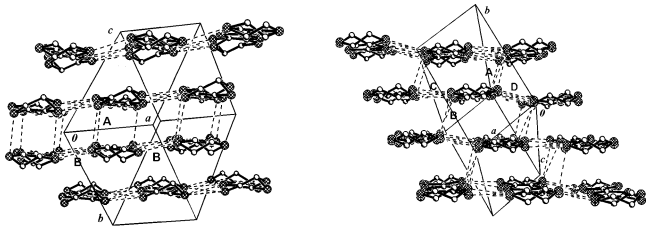

Figure 3. View along the long axis of BEDT-TTF radical cations of the BEDT-TTF arrangements in the $(BEDT\text{-}TTF)_2[(IBr_2)_{0.2}(BrICl)_{0.1}(ICl_2)_{0.7}]$ salt: (left) *β′*-phase and (right) *β″*-phase.

On the other hand, X-ray data show that the unit cell parameters of **2** and **3** are different: the former is isostructural to the *β′*-$(BEDT\text{-}TTF)_2ICl_2$ salt reported by Buravov et al.,[17] while the latter is isostructural to the *β″*-phases of BEDT-TTF-based salts with linear anions ICl_2^-,[17] $AuBr_2^-$,[24] $IAuBr^-$,[25] and $Br_{1.3}I_{1.1}Cl_{0.6}^-$.[13] Therefore, these data confirm that two polymorphs of the new $BEDT\text{-}TTF_2[(IBr_2)_{0.2\pm\delta}(BrICl)_{0.1\pm\delta}(ICl_2)_{0.7\pm\delta}]$ salt can be generated from a solution containing the above mixture of anions. Hereafter for simplicity we will use the formula $(BEDT\text{-}TTF)_2[(IBr_2)_{0.2}(BrICl)_{0.1}(ICl_2)_{0.7}]$. These two crystal modifications contain BEDT-TTF layers separated by anion layers in which all trihalide anions are located on inversion centers (Figure 2). The layers are alternate along the *c* direction. The interstack BEDT-TTF topology[3] with inversion centers located between stacks is also characteristic of both polymorphs (Figure 2). But there are some principal structural distinctions in the intrastack BEDT-TTF arrangements between the two polymorphs.

The BEDT-TTF arrangements in **2** and **3** form different S···S networks (Figure 3, see the Supporting Information), hence forming various electronic states:

(24) Mori, T.; Sakai, F.; Saito, G.; Inokuchi, H. *Chem. Lett.* **1986**, 1037.
(25) Ugawa, A.; Kuroda, K.; Kawamoto, A.; Tanaka, J. *Chem. Lett.* **1986**, 1875.
(26) Emge, T. J.; Wang, H. H.; Leung, P. C. W.; Rust, P. R.; Cook, J. D.; Jackson, P. L.; Karlson, K. D.; Williams, J. M.; Whangbo, M.-H.; Venturini, E. L.; Schirber, J. E.; Azevedo, L. J.; Ferraro J. R. *J. Am. Chem. Soc.* **1986**, *108*, 695.

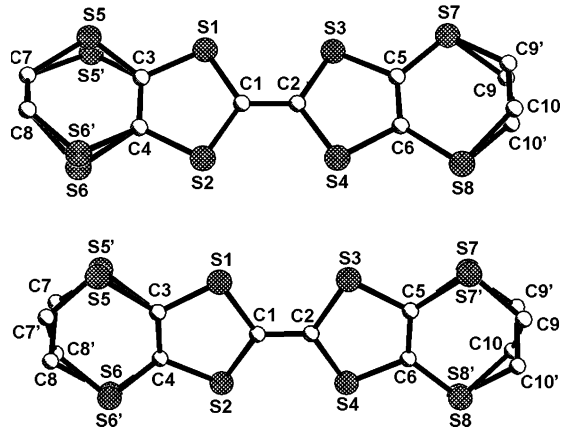

Figure 4. Labeling scheme for the BEDT-TTF molecule in $(BEDT\text{-}TTF)_2[(IBr_2)_{0.2}(BrICl)_{0.1}(ICl_2)_{0.7}]$: (top) β'-phase and (bottom) β''-phase.

2 (β'-phase) is semiconducting, while **3** (β''-phase) is metallic down to He temperatures (see below).

As the structural peculiarities of both phase types have already been discussed[17] we will concentrate on a subtle adjustment of the β'-, β''-BEDT-TTF conducting layers by the above mixture of anions. We discovered in both polymorphs a disorder in the BEDT-TTF layer that was not observed for the β'- and β''-$(BEDT\text{-}TTF)_2ICl_2$ salt.[17]

Thus, the adjustment of the β'-BEDT-TTF layer results in a disorder of the ethylene group of one of the two six-membered rings of the BEDT-TTF molecule and a weak disorder of both S atoms located in the other ring, the occupancies of S(5′) and S(6′) being 0.035(10) and 0.060(7), respectively (Figure 4, top). The response of the β''-BEDT-TTF layer leads to a disorder of both terminal ethylene groups and a weak disorder of one of the S atoms, which are located in the six-membered rings of BEDT-TTF: the occupancies of S(5′) and S(6′) are 0.130(5), and those of S(7′) and S(8′) are 0.300(6) (Figure 4, bottom). Meanwhile, in the isostructural $(BEDT\text{-}TTF)_2ICl_2$ salt there is no disorder in the β'-phase, and only one terminal ethylene group is disordered in β''-BEDT-TTF layers.[17]

Electrical Properties. In what follows we will consider how the structural adjustment of the β'- and β''-BEDT-TTF conducting layers of the new trihalide salt relates to transport properties of its polymorphs.

The room-temperature conductivity of **2** (β'-phase), when the current is running parallel to the BEDT-TTF radical cation layers ($\sigma_{||}$) was measured to be $\sim 2 \times 10^{-2}$ S cm^{-1}, the $R(T)$ demonstrating semiconductor-like behavior (Figure 5). The activation energy value was found to be 0.076 eV. This value is remarkably lower than that reported for isostructural β'-$(BEDT\text{-}TTF)_2ICl_2$ crystals.[17] This effect results from the disorder revealed in semiconductor layers of **2** (β'-phase).

The room-temperature conductivity of the β''-single crystal (**3**) in the conducting *ab*-plane amounts to 10−50 S cm^{-1}. This value is lower than that reported for the β''-$(BEDT\text{-}TTF)_2ICl_2$ crystal ($\sigma_{||} = 200$ S cm^{-1}).[17] The temperature dependence of the resistance of **3** is metal-like within the temperature range 10−293 K (Figure 6). Below 10 K, the resistance increases slightly (see inset in Figure 6), most probably resulting from a localization of carriers, which can be provoked at low

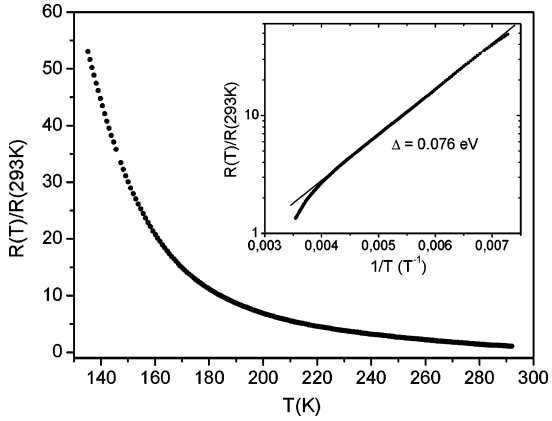

Figure 5. Temperature dependence of normalized resistance for the β'-$(BEDT\text{-}TTF)_2[(IBr_2)_{0.2}(BrICl)_{0.1}(ICl_2)_{0.7}]$ (**2**) crystal; the inset shows a plot of the logarithm of the resistance versus inverse temperature.

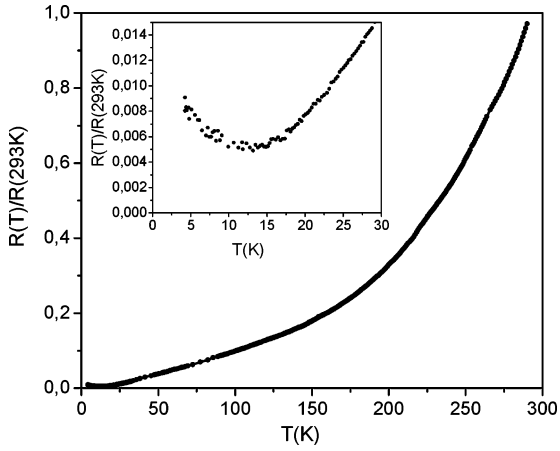

Figure 6. Temperature dependence of normalized resistance for the β''-$(BEDT\text{-}TTF)_2[(IBr_2)_{0.2}(BrICl)_{0.1}(ICl_2)_{0.7}]$ crystal; the inset shows the low-temperature region.

temperature by the disorder in the β''-BEDT-TTF layers. The overall decrease of the resistance R_{293K}/R_{10K} was found to be ∼200. It should be note that the localization was not observed for isostuctural β''-$(BEDT\text{-}TTF)_2ICl_2$ crystals down to 1.5 K.[17]

Therefore, summing up the experimental data, one can see that the adjustment of both BEDT-TTF systems by the mixture of C−H···Cl−I−Cl$^-$ (≈75%) and C−H···Br−I−Y$^-$ (Y = Br, Cl) (≈25%) interactions remarkably affects their transport properties.

Room-Temperature ESR Studies. We studied the anisotropy of the ESR signal of the single crystals of both polymorphs at room temperature. Crystals were rotated in three orthogonal planes, corresponding to the *ab*, *bc*, and *ac* crystallographic planes. The maximum, intermediate, and minimum values of the *g*-factor and peak-to-peak line width (ΔH_{pp}) for both phases are listed in Table 4.

The semiconductor β'-phase shows the narrower line width (12−9.7 G) when compared with the metallic β''-polymorph ($\Delta H_{pp} = 56-43$ G). This indicates a reduction in dimensionality of the β'-phase from that of the β''-phase.[3] These results are in accordance with the X-ray data revealing a smaller number of short S···S contacts between interstack BEDT-TTF molecules in the β'-phase in relation to that in the β''-polymorph (see Figure 3 and Supporting Information).

Table 4. *g*-Factor and Peak-to-Peak Line Width (ΔH_{pp}) of the ESR Signal for Different Crystal Samples of the $(BEDT\text{-}TTF)_2[(IBr_2)_{0.2}(BrICl)_{0.1}(ICl_2)_{0.7}]$ Salt at Room Temperature

crystal type, phase	parameters of the EPR signal					
	maximum		intermediate		minimum	
	g	ΔH_{pp}, G	g	ΔH_{pp}, G	g	ΔH_{pp}, G
2, β'	2.0074	12	2.0037	10.5	2.0029	9.7
3, β''	2.0114	56	2.0045	45	2.0021	43
4, β''	2.0112	56.6	2.0049	44	2.0020	44
3, β^a	2.0099	24	2.0062	22.3	2.0028	19.4

[a] ESR parameters of crystal **3** after its annealing at 443 K during 20 min.

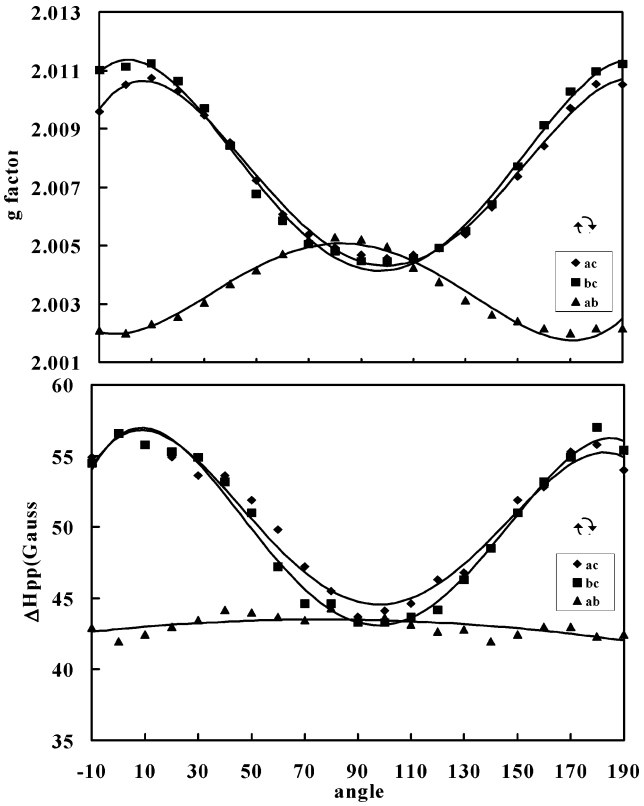

Figure 7. Angular dependence of (top) *g*-factor and (bottom) ESR line width (ΔH_{pp}) for the β''-$(BEDT\text{-}TTF)_2[(IBr_2)_{0.2}(BrICl)_{0.1}(ICl_2)_{0.7}]$ crystal at room temperature for three different orthogonal rotation planes.

The angular dependence of ESR parameters of the β''-phase (*g*-factor and ΔH_{pp}) for the three orthogonal rotation planes is presented in Figure 7. The values of both parameters are practically constant when the magnetic field is applied parallel to the *ab* plane of the crystal. However, a considerable anisotropy with a sinusoidal dependence is observed for these parameters in the other two rotation planes. Thus, the angle dependence of the ESR signal for this phase indicates some isotropic electronic structure in the *ab* plane and a strongly anisotropic one in the *ac* and *bc* planes; in fact, this is characteristic of a quasi-2D organic metal. Therefore, the network of S···S contacts (Figure 3, right) of the β''-phase, is sufficient to promote the pronounced 2D character of its electronic structure.

Transformations of Metallic β''-BEDT-TTF Layer. As the $(BEDT\text{-}TTF)_2[(IBr_2)_{0.2}(BrICl)_{0.1}(ICl_2)_{0.7}]$ salt exists in two phases, the question of mutual phase transitions is raised. Taking into account that the peak-to-peak line width of the ESR signal is a useful parameter for the identification of small crystals of different phases of BEDT-TTF trihalides and the investigation of their various phase transformations at high or low temperature,[3,11−13,25] we applied ESR spectroscopy for studying temperature-dependent structural transformations of the β'- and β''-$(BEDT\text{-}TTF)_2[(IBr_2)_{0.2}(BrICl)_{0.1}(ICl_2)_{0.7}]$ phases.(X-ray powder diffraction and TG/DTA measurements cannot be applied for studying temperature-dependent structural transformations of the $(BEDT\text{-}TTF)_2[(IBr_2)_{0.2}(BrICl)_{0.1}(ICl_2)_{0.7}]$ salt because this salt may be obtained in reasonable quantity as a mixture of very small crystals of two phases; typical crystal dimensions are 1 × 0.3 × 0.002 mm.)

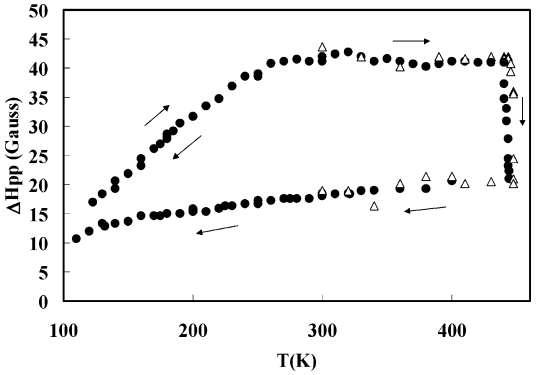

Figure 8. Temperature dependence of the ESR line width (ΔH_{pp}) for the β''-$(BEDT\text{-}TTF)_2[(IBr_2)_{0.2}(BrICl)_{0.1}(ICl_2)_{0.7}]$ crystal. Different symbols correspond with two different crystals. The static magnetic field was oriented parallel to the conducting (*ab*) plane.

We studied the temperature dependence of the ESR signal of the single crystals in the range from 115 to 450 K, when the static magnetic field was oriented parallel to the conducting (*ab*) plane. Crystals were heated and cooled in nitrogen gas at 10 K intervals.

The ESR line width as a function of temperature for the β''-phase is shown in Figure 8. When the crystal of the β''-phase is heated from 115 to 260 K the peak-to-peak line width linearly increases from 16 to 43 G. The slope of $\Delta H_{pp}(T)$, which is related to electron scattering rate, is nearly identical for the metallic β-, α-, and θ-BEDT-TTF salts.[3] This phenomenon correlates the relaxation rate with torsional oscillations of the organic donor molecule.[3] The ΔH_{pp} value is temperature independent in the range 260−440 K, which is not typical for the metallic BEDT-TTF systems. At high temperature (>440 K), an irreversible change of the line width for the β''-phase crystal takes place: it jumps down from ∼40 to ∼20 G (Figure 8). The change occurs under the crystal annealing at 443 K during 20 min (warm nitrogen gas). We studied several β''-phase crystals of the new salt and all of them demonstrate the same change of their ESR signals above 440 K; the $\Delta H_{pp}(T)$ data at high-temperature cycle for another β''-phase crystal are also presented in Figure 8. To determine the type of BEDT-TTF layer formed at high temperature, one of the thermally converted crystals was rotated in three orthogonal planes (see Table 4). These ESR data (*g*-factor and ΔH_{pp}) are the typical ones for the superconducting β-phases of $(BEDT\text{-}TTF)_2X$ (X = I_3, IBr_2, AuI_2).[3,4,11] Therefore, the ESR data demonstrate that

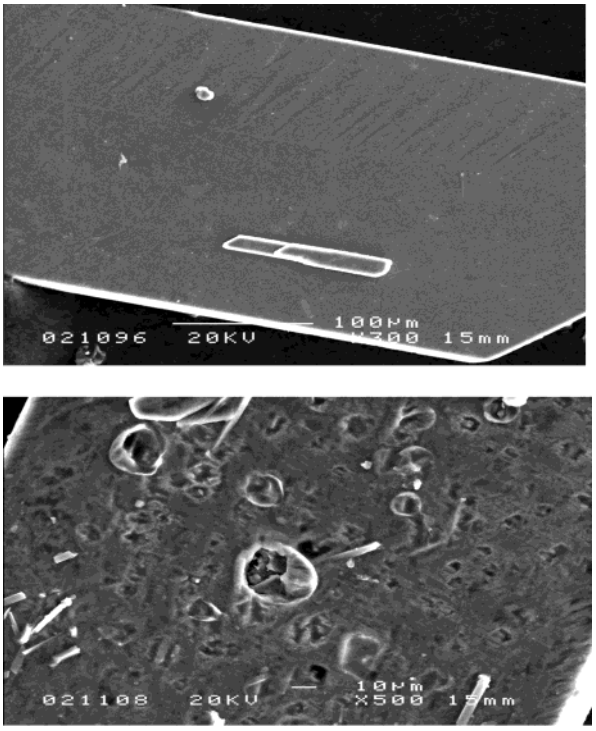

Figure 9. SEM image of the surface of the β''-$(BEDT\text{-}TTF)_2[(IBr_2)_{0.2}(BrICl)_{0.1}(ICl_2)_{0.7}]$ crystal: (top) before and (bottom) after the thermocycle (293 → 443 → 293 K).

Scheme 1

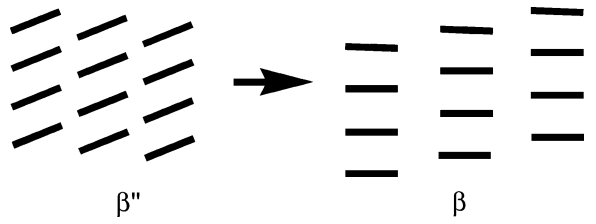

Table 5. Microanalysis Data on a Halide Atom Contribution for Two Different Parts of the Crystal of the β''-, β'-$(BEDT\text{-}TTF)_2[(IBr_2)_{0.2}(BrICl)_{0.1}(ICl_2)_{0.7}]$ Salt before and after Thermocycle: 293 → 445 → 293 K

	halide atoms' contribution							
	before thermocycle				after thermocycle			
	atomic %				atomic %			
crystal	Br	I	Cl	$Br_xI_yCl_z$	Br	I	Cl	$Br_xI_yCl_z$
β''	19.2	34.1	46.7	$Br_{0.6}I_{1.0}Cl_{1.4}$	26.8	73.2		$Br_{0.8}I_{2.2}$
	17.8	36.8	45.4	$Br_{0.5}I_{1.1}Cl_{1.4}$	25.0	75.0		$Br_{0.8}I_{2.2}$
β'	16.5	35.7	47.8	$Br_{0.5}I_{1.1}Cl_{1.4}$	25.2	62.5	12.4	$Br_{0.7}I_{1.9}Cl_{0.4}$
	17.3	34.6	48.2	$Br_{0.5}I_{1.0}Cl_{1.5}$	21.3	53.5	25.2	$Br_{0.6}I_{1.6}Cl_{0.8}$

above 440 K the $\beta'' \rightarrow \beta$ transformation takes place; the changing of the conducting BEDT-TTF layer may be represented schematically as in Scheme 1.

The SEM study (Figure 9) shows that although the thermally converted crystals hold their original shapes, their surfaces are very imperfect. Due to the high mosaicity of the thermally converted crystals, it was not possible to perform X-ray studies.

A microanalytical study (Table 5) of different parts of the thermally converted crystals demonstrates (i) the absence of Cl atoms in dark (conducting) parts of the crystal surface (see Figure 9), the contribution of Br and I atoms being $I_{2.2\pm0.1}Br_{0.8\pm0.1}$ and (ii) the absence of all halogen atoms in light parts of the crystal surface (Figure 9), with the contribution of C and S atoms being very close to that expected for BEDT-TTF molecules.

Therefore, at high temperature ($T \cong 443$ K) the anion layer decomposes, resulting in the formation of a new BEDT-TTF trihalide salt in which BEDT-TTF radical cations have the β-type arrangement. This superconducting β-type BEDT-TTF arrangement is well-known as the most thermodynamically stable in BEDT-TTF systems.[3]

The high temperature (HT) decomposition of $[(IBr_2)_{0.2}(BrICl)_{0.1}(ICl_2)_{0.7}]$ anion brings up the question of what halides are formed during this process. It is likely that the HT decomposition of $[(IBr_2)_{0.2}(BrICl)_{0.1}(ICl_2)_{0.7}]$ anion is analogous to the process found for the HT $\alpha' \rightarrow \beta$ transformation of the nanocrystalline layer of $(BEDT\text{-}TTF)_2(I_xBr_{1-x})_3$.[12] In such an event, the HT decomposition of the anion should lead to (i) generation of neutral ICl(IBr) and BEDT-TTF molecules and (ii) formation of a new most thermodynamic stable BEDT-TTF trihalide salt via BEDT-TTF + ICl(IBr) reaction. This process can be represented schematically as

$$\beta''\text{-}(BEDT\text{-}TTF)_2[(IBr_2)_{0.2}(BrICl)_{0.1}(ICl_2)_{0.7}]$$

$$\downarrow$$

$$BEDT\text{-}TTF + IBr + ICl;\ ICl >> IBr$$

$$\downarrow$$

$$\beta\text{-}(BEDT\text{-}TTF)_2Br_{0.8\pm0.1}I_{2.2\pm0.1}$$

From the anion stoichiometry it should be assumed that the HT decomposition of the $[(IBr_2)_{0.2}(BrICl)_{0.1}(ICl_2)_{0.7}]^-$ anion results in the formation of ICl as the main component. Therefore, we suggest that the $(BEDT\text{-}TTF)_2I_3$ salt can be formed via the BEDT-TTF + ICl reaction. Taking into account that the contribution of each trihalide anion formed during the oxidation of BEDT-TTF by ICl may depend on the polarity of the environment,[12] we have performed the BEDT-TTF + ICl reaction in trichloromethane (the model of a weakly polar environment) and in nitrobenzene (the model of a strongly polar environment). The crystals obtained were characterized by EDX, X-ray, Raman, and ESR. Crystals grown in trichloromethane were characterized as β- and κ-$(BEDT\text{-}TTF)_2I_3$, whereas those obtained in nitrobenzene were characterized as β-$(BEDT\text{-}TTF)_2I_{2.45}Cl_{0.55}$, β'-$(BEDT\text{-}TTF)_2I_{1.1}Cl_{1.9}$, and β''-$(BEDT\text{-}TTF)_2I_{1.25}Cl_{1.75}$. Since the HT transformation in crystals of β''-$(BEDT\text{-}TTF)_2[(IBr_2)_{0.2}(BrICl)_{0.1}(ICl_2)_{0.7}]$ was studied in nitrogen gas, the experimental data on the oxidation of BEDT-TTF by ICl in a weakly polar environment, which show the formation of $(BEDT\text{-}TTF)_2I_3$ salt, are in a good agreement with the process suggested above.

We found further evidence of this HT process when we performed the ESR study of the isostructural β''-$(BEDT\text{-}TTF)_2ICl_2$ crystals. At high temperature ($T >$ 370 K) we observed a drastic change of the ESR line width of the β''-$(BEDT\text{-}TTF)_2ICl_2$ single crystal (Figure 10).

Similarly to the peak-to-peak line width of the β''-$(BEDT\text{-}TTF)_2[(IBr_2)_{0.2}(BrICl)_{0.1}(ICl_2)_{0.7}]$ crystals, the peak-to-peak line width of the β''-$(BEDT\text{-}TTF)_2ICl_2$ crystal

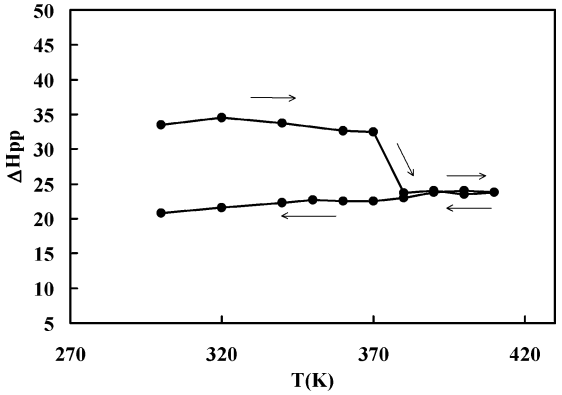

Figure 10. Temperature dependence of the ESR line width (ΔH_{pp}) for the β''-(BEDT-TTF)$_2$ICl$_2$ crystal. The static magnetic field was oriented parallel to the conducting (*ab*) plane.

Scheme 2

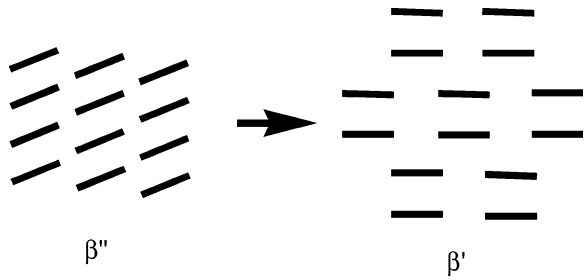

also falls down from ~35 G to ~20 G. The thermally converted crystal was rotated in three orthogonal planes. The parameters of its ESR signal (*g*-factor = 2.0097−2.0030 and ΔH_{pp} = 23-21 G) are the typical ones for the well-known β-(BEDT-TTF)$_2$I$_3$.[3] The microanalysis study of different parts of the thermally converted β''-(BEDT-TTF)$_2$ICl$_2$ crystal also shows the absence of Cl atoms and gives the atomic contribution of C, S, and I as 52%, 41%, and 7%, respectively; these values are very close to the theoretical ones for the β-(BEDT-TTF)$_2$I$_3$ salt: C = 51.3%, S = 41.0%, and I = 7.7%.

This result provides the basic evidence in supporting of the solid-state reactions presented above. The $\beta'' \rightarrow \beta$ transformation of the β''-(BEDT-TTF)$_2$ICl$_2$ crystals can be represented schematically as

β''-(BEDT-TTF)$_2$ICl$_2$

↓

BEDT-TTF+ ICl;

↓

β-(BEDT-TTF)$_2$I$_3$

Compared to the β''-(BEDT-TTF)$_2$[(IBr$_2$)$_{0.2}$(BrICl)$_{0.1}$(ICl$_2$)$_{0.7}$] crystals, the transformation of the β''-(BEDT-TTF)$_2$ICl$_2$ phase occurs about 70 K lower. This result points to the fact that the increasing of the softness of the lattice of the β''-phase by substitution of 25% of the C−H···Cl−I−Cl$^-$ interactions for the weaker C−H···Br−I−Y$^-$ (Y = Br, Cl) ones[3,16] significantly prevents a decomposition of this type of the BEDT-TTF arrangement from amplification of the lattice vibrations at high temperature.

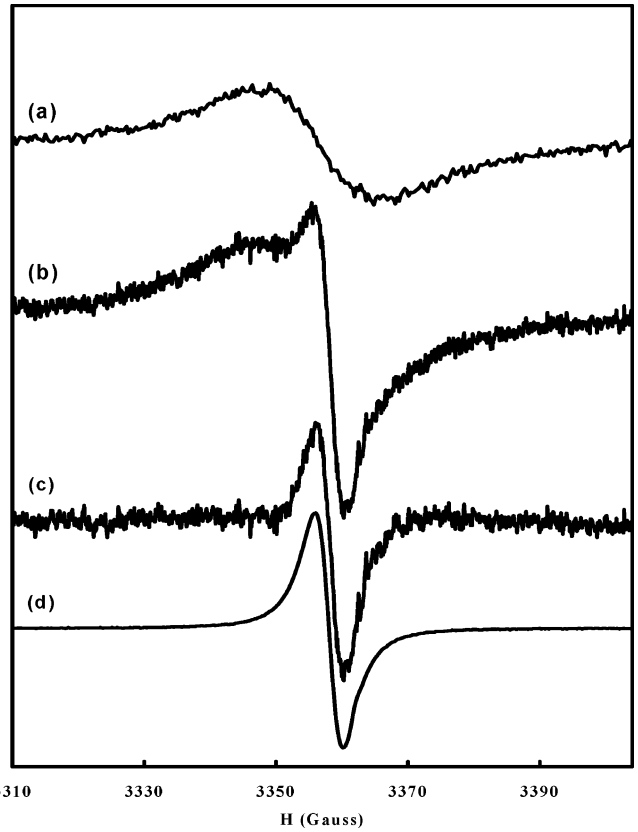

Figure 11. The ESR spectra at T = 140 K of the β''-(BEDT-TTF)$_2$[(IBr$_2$)$_{0.2}$(BrICl)$_{0.1}$(ICl$_2$)$_{0.7}$] crystal after being heated to 440 K (before the solid-state reaction) evidencing the partial β'' to β' transformation: (a) as soon as the crystal was heated to 440 K and cooled from 440 to 140 K; (b) six months after keeping of the crystal at room temperature; (c) subtraction of spectra a from b; (d) the ESR spectrum of the β'-(BEDT-TTF)$_2$-[(IBr$_2$)$_{0.2}$(BrICl)$_{0.1}$(ICl$_2$)$_{0.7}$] crystal at 140 K.

The partial $\beta'' \rightarrow \beta'$ transformation (Scheme 2) was also discovered in the (BEDT-TTF)$_2$[(IBr$_2$)$_{0.2}$(BrICl)$_{0.1}$-(ICl$_2$)$_{0.7}$] salt.

Indeed, we have observed that the ESR spectrum of the β''-crystal, which was heated to 440 K (before the solid state reaction) and then cooled to 115 K and heated to the room temperature, varied considerably in six months.

The new ESR spectrum studied at 140 K consists of two different ESR signals (Figure 11b): a broad dominant signal (ΔH_{pp} = 20 G, g = 2.0037) and a new narrow signal (ΔH_{pp} = 4.4 G, g = 2.0020). The former is characteristic of the initial β''-phase at T = 140 K (Figure 11a), while the latter is typical of the β'-phase at the same temperature (Figure 11d). These ESR data allow us to imagine this crystal of (BEDT-TTF)$_2$[(IBr$_2$)$_{0.2}$-(BrICl)$_{0.1}$(ICl$_2$)$_{0.7}$] as a mixture of the polymorphs: β''(90%) and β'(10%). Under a second heating cycle from 293 K up to 445 K, at ~442 K we found a drastic change of the ESR peak-to-peak line width, which was identical to that during the $\beta'' \rightarrow \beta$ phase transformation.

For the β'-phase of (BEDT-TTF)$_2$[(IBr$_2$)$_{0.2}$(BrICl)$_{0.1}$-(ICl$_2$)$_{0.7}$] the ΔH_{pp} value monotonically increases from 3.8 G at 115 K to 10.4 G at 445 K, but there are not any sudden changes in the ESR line width (Figure 12).

However, above 430 K the intensity of the ESR signal of the β'-phase starts to decrease rapidly. The analysis

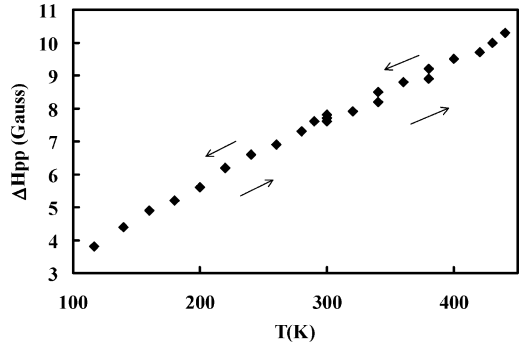

Figure 12. Temperature dependence of the ESR line width (ΔH_{pp}) for the β'-(BEDT-TTF)$_2$[(IBr$_2$)$_{0.2}$(BrICl)$_{0.1}$(ICl$_2$)$_{0.7}$] crystal.

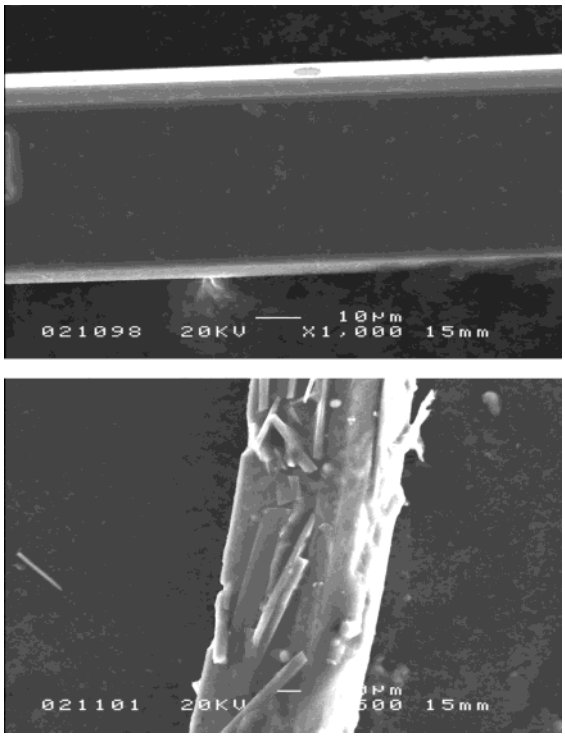

Figure 13. SEM image of the surface of the β'-(BEDT-TTF)$_2$[(IBr$_2$)$_{0.2}$(BrICl)$_{0.1}$(ICl$_2$)$_{0.7}$] crystal: (top) before and (bottom) after the thermocycle 293 → 445 → 293 K.

of the SEM images of the β'-phase crystal before (Figure 13, top) and after the 293 → 445 → 293 K thermocycle (Figure 13, bottom) clearly indicates that at high temperature the β'-crystal is decomposed, resulting in a formation of new microcrystals. The data presented in Table 5 show a depletion of the crystal in Cl, the various parts of the crystal differing in the halide stoichiometry.

In contrast to the β''-phase, we cannot obtain any evidence of the $\beta' \rightarrow \beta$ transformation; at annealing of the β' -phase at 445 K during 60 min, we observed a drastic decrease of the ESR intensity but not any change of the peak-to-peak line width.

The theory of the high-temperature transformations in BEDT-TTF trihalides is not sufficiently advanced to explain the difference of the high-temperature behavior of two polymorphs of the new BEDT-TTF-based salt. It is probable that strong interactions inside of the BEDT-TTF dimers of the β'-phase interfere with the transformation to the β-type BEDT-TTF arrangement.

Summary

The original aspect of this study is to show that the mixture of anions IBr_2^- (≈20%), $BrICl^-$ (≈10%), and ICl_2^- (≈70%) can be successfully integrated in the architecture of molecular crystals with semiconducting β'- or metallic β''-BEDT-TTF layers; the fine adjustment of both BEDT-TTF arrangements by the C−H···Cl−I−Y$^-$ (≈75%) and C−H···Br−I−Y$^-$ (≈25%) interactions results in a disorder of their BEDT-TTF molecules and in turn has a great influence on their transport properties.

The HT $\beta'' \rightarrow \beta$ and partial $\beta'' \rightarrow \beta'$ transformations were discovered for the first time in BEDT-TTF-based salts and studied by ESR spectroscopy and EDX analysis. The ESR studies show that the increasing of the lattice softness of the metallic β''-phase by substitution of some C−H···Cl−I−Cl$^-$ interactions for the weaker C−H···Br−I−Y$^-$ (Y = Cl, Br) ones might significantly stabilize this type of the BEDT-TTF arrangement at high temperature. These results could provide a novel approach for understanding and designing of new conducting molecular materials.

Acknowledgment. We are grateful to Dr. E. Yudanova for help with numerous crystal testing by means of their ESR spectra at room temperature. This work was supported by DGI-Spain (BQU2003-00760), by Generalitat de Catalunya (2000 SGR-00114), and by the Polish State Committee for Scientific Research (grant No 7 T08A 01320). E.L. is grateful to NATO for the DC type grant.

Supporting Information Available: CIF files of the X-ray structures of the β'- and β''-(BEDT-TTF)$_2$[(IBr$_2$)$_{0.2}$(BrICl)$_{0.1}$(ICl$_2$)$_{0.7}$] polymorphs; tables of S···S contacts for the two structures (PDF). This material is available free of charge via the Internet at http://pubs.acs.org.

CM034866Q